IOP Publishing Environ. Res. Lett. 16 (2021) 044003 https://doi.org/10.1088/1748-9326/abe9ed

ENVIRONMENTAL RESEARCH
LETTERS

OPEN ACCESS

RECEIVED
21 September 2020

REVISED
22 February 2021

ACCEPTED FOR PUBLICATION
25 February 2021

PUBLISHED
11 March 2021

LETTER

Defining El Niño indices in a warming climate

Geert Jan van Oldenborgh[1,*], Harry Hendon[2], Timothy Stockdale[3], Michelle L'Heureux[4], Erin Coughlan de Perez[5,6,7], Roop Singh[5] and Maarten van Aalst[5,7,8]

[1] Koninklijk Nederlands Meteorologisch Instituut, De Bilt, Netherlands
[2] Bureau of Meteorology Research Centre, Melbourne, Australia
[3] European Centre for Medium Range Weather Forecasts, Reading, United Kingdom
[4] NOAA Climate Prediction Center, College Park, MD, United States of America
[5] Red Cross Red Crescent Climate Centre, The Hague, The Netherlands
[6] Institute for Environmental Studies, VU University Amsterdam, The Netherlands
[7] International Research Institute for Climate and Society, Earth Institute, Columbia University, Palisades, NY, United States of America
[8] Faculty of Geo-information Science and Earth Observation, University of Twente, Enschede, The Netherland
[*] Author to whom any correspondence should be addressed.

E-mail: oldenborgh@knmi.nl

Keywords: El Niño, Niño3.4 index, global warming, teleconnections, disaster preparedness

Abstract

Extreme weather and climate events associated with El Niño and La Niña cause massive societal impacts. Therefore, observations and forecasts are used around the world to prepare for such events. However, global warming has caused warm El Niño events to seem bigger than they are, while cold La Niña events seem smaller, in the commonly used Niño3.4 index (sea surface temperature (SST) anomalies over 5° S–5° N, 120–170° W). We propose a simple and elegant adjustment, defining a relative Niño3.4 index as the difference between the original SST anomaly and the anomaly over all tropical oceans (20° S–20° N). This relative index describes the onset of convection better, is not contaminated by global warming and can be monitored and forecast in real-time. We show that the relative Niño3.4 index is better in line with effects on rainfall and would be more useful for preparedness for El Niño and La Niña in a changing climate and for El Niño—Southern Oscillation research.

1. Introduction

The greatest source of seasonal climate variability is the El Niño—Southern Oscillation (ENSO), which drives changes in rainfall and surface temperatures worldwide (van Oldenborgh *et al* 2005). ENSO forecasts provided by WMO global producing centers (GPCs) are used to inform regional and national forecasts and associated advisories and are routinely used by a wide range of users around the world to anticipate climate fluctuations, for instance in agriculture, public health, water management, and commodity markets.

A key role is played by ENSO indices, which are used to monitor events in order to determine when an ENSO event is 'declared.' These declarations are often the trigger for early action in anticipation of expected climate conditions. For instance, in 2015, Kenyan forecasters took note of the 'strong El Niño' forecasted by GPCs and alerted the general public and appropriate government ministries. Advisories went out, for instance, to the health and agriculture sectors to plan for flooding and reduce potential impacts. In addition to government action, humanitarian organizations such as the Red Cross mobilized early actions to limit possible damage. Despite the imperfect correlation between the strength of El Niño, extreme event teleconnections, and humanitarian impacts, people often conflate these parameters and act more readily when the event is declared 'strong.' In this case, Kenya-wide precipitation indeed turned out to be 35% above average, but only a few local extreme precipitation events caused damage.

Following the 2015/16 'strong' El Niño, conditions more similar to La Niña appeared. However, GPCs disagreed on whether there would be an event and whether its strength would be greater than 'weak.' As a result, forecasters in East Africa were reluctant to provide strong advisories to key actors in the region. The following drought across the Horn of Africa, although only partly attributable to La Niña (Uhe *et al* 2018), was poorly anticipated, and is estimated

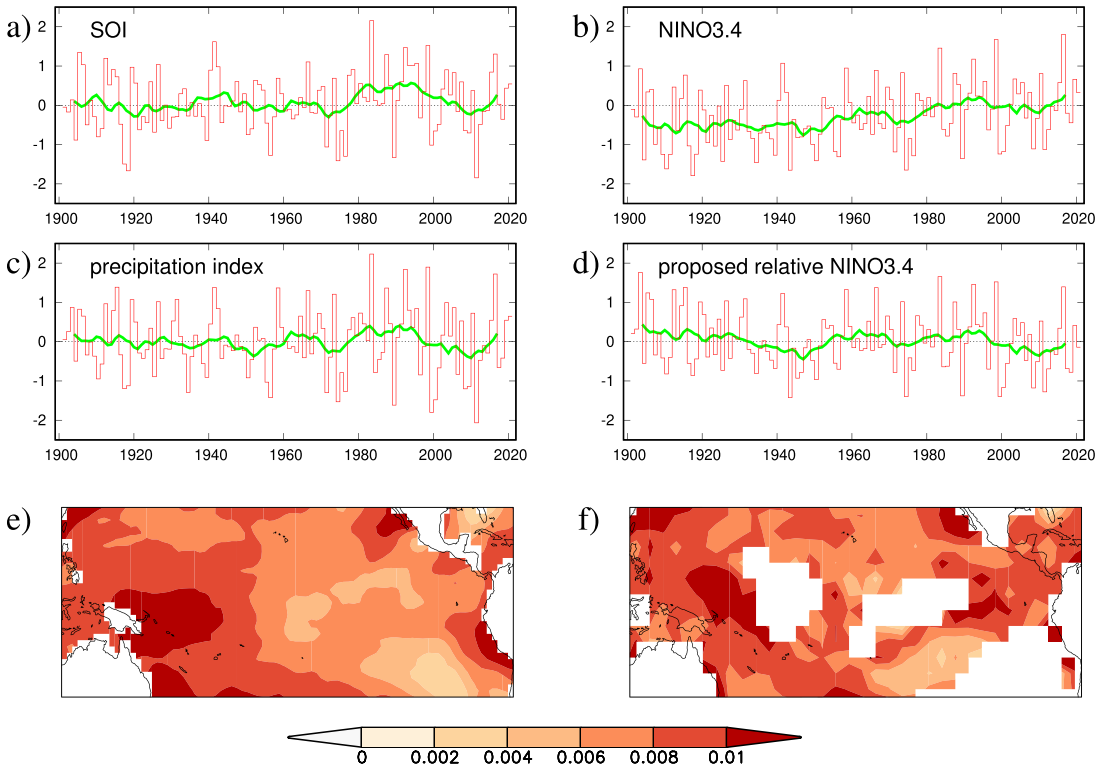

Figure 1. Ten-year running means (green) of July–June averaged ENSO indices (red) 1900/01–2019/20, as well as the detrended index proposed here. (a) SOI index from CRU (Allan *et al* 1991, Können *et al* 1998) (multiplied by −1 so that El Niño is positive, La Niña negative). (b) Niño3.4 index (K) based on ERSST v5 (Huang *et al* 2017). (c) Index reconstructed from GPCC precipitation analyses (Schneider *et al* 2018) using monthly Niño3.4 teleconnections (K). (d) Relative Niño3.4 index (K) proposed in this paper, based on ERSST v5. (e) Trend in the tropical Pacific 1900–2020 (K/ppm) in the ERSST v5 dataset and (f) HadSST4 dataset.

to have affected 26.5 million people by June 2017 (Office for the Coordination of Humanitarian Affairs (OCHA) 2017).

In this paper, we demonstrate that the 'extremely strong' categorization of the 2015/16 El Niño and the 'weak' categorization of the 2016 La Niña may have put both forecasters and users on the wrong footing. The cause is a contamination of the main ENSO index by a long-term warming trend from climate change.

We propose a relative index that does not have this trend. This relative index would indeed have provided better information on actual ENSO conditions in these El Niño and La Niña events. In addition, the relative index would have remained neutral in 2019/20, when the regular Niño3.4 index indicated El Niño conditions, but the atmospheric circulation was closer to neutral. Of course as with any ENSO index there will also still be cases where climate conditions do not fully follow the index: El Niño is not a simple, one-dimensional phenomenon that is completely described by a single number.

2. ENSO indices

The oldest ENSO index is the Southern Oscillation Index (SOI, Walker 1924). It is the normalized surface pressure difference between the tropical Central Pacific and West Pacific. The two stations in these regions with the best records are Tahiti and Darwin, so the station-based definition uses mainly these (Allan *et al* 1991, Können *et al* 1998). NOAA CPC also defines an Equatorial SOI based on the pressure difference across the Pacific from the NCEP/NCAR R1 reanalysis 1948–now, but the two series are very similar ($r = 0.96$ for monthly values 1948–2020).

Figure 1(a) shows the station-based July–June annual means of the SOI (multiplied by −1 so that El Niño is positive and La Niña is negative), together with a 10 year running mean. The July–June means capture the lifetimes of El Niño and La Niña events, which typically peak in Boreal winter (Tippett and L'Heureux 2020). The series has a small, non-significant trend toward El Niño, mainly caused by two large and several small El Niño events in 1982–1998. The ten-year running mean has since reverted to zero.

However, the SOI is a measure of the atmospheric anomaly, but ENSO is a coupled ocean-atmosphere vacillation. Ocean surface temperatures in the equatorial Pacific are used to directly monitor the strength of ENSO from an oceanic perspective and are more directly indicative of the anomalous forcing of the atmosphere during ENSO, with the atmosphere not only responding to sea surface temperature (SST) patterns but also generating weather noise internally.

Several SST-based ENSO indices were defined at the Climate Diagnostics Center following the ship-track analysis by Rasmusson and Carpenter (1982). Niño1+2 describes warming close to the South American coast ('coastal El Niño'), which is relevant for heavy rain on the Ecuadorian and Peruvian coast (like in February–March 2017), but only loosely coupled ($r = 0.5$ monthly) to the larger-scale warming along the equator in the eastern-central Pacific Ocean ('basin El Niño') that affects the weather in the rest of the world. All other indices are defined on the equatorial wave guide 5° S–5° N. Niño3 (90–150° W) covers the cold tongue region and Niño4 (160° E–150° W) the edge of the warm pool.

Later research (e.g. Barnston *et al* 1997) showed that a region between Niño3 and Niño4 is best correlated to many global teleconnections. This region, 120°–170° W, was named Niño3.4 and is now the most widely used index to monitor the strength of El Niño and La Niña (Horsfall 2006). NOAA provides a widely-used set of Niño indices based on the ERSST v5 analysis (Huang *et al* 2017) from 1950–now. Values from 1854 based on the same dataset, with larger uncertainties going further back in time, are available from, e.g. the KNMI Climate Explorer (see figure 1(b)).

These indices are used extensively because of the much lower influence of weather noise, which implies that they have a better signal/noise ratio, and hence predictability, than the SOI. Forecasts of the Niño indices, and particularly Niño3.4, are also frequently used as an early indication of global climate and weather patterns in the upcoming months based on past teleconnections. Forecast plumes of these indices are provided from dynamical seasonal forecast models run at, for instance, ECMWF and Australian Bureau of Meteorology, and forecasts from multiple models are provided by, for instance, Copernicus, the North American multi-model ensembles, and IRI/CPC. The indices are also used to explain and interpret dynamical forecasts and hence increase trust in them.

3. Trends in ENSO indices

The problem is that the observed Niño3.4 series has a clear trend (even disregarding the less-reliable first few decades), as shown in figure 1(b) (e.g. L'Heureux *et al* 2013). To quantify it we prefer not to use a linear trend, as the warming trend since the industrial era has accelerated over the last 50 years. We therefore define the trend as the regression on the observed CO_2 concentration (Etheridge *et al* 1996, Ballantyne *et al* 2012). The annual global mean temperature has a correlation of $r = 0.94$ with this measure over 1880–2018, given that other forcings such as aerosols are to a large extent proportional to the CO_2 concentration (Suckling *et al* 2016), so a regression on the global mean temperature or another index that has the same rough shape gives very similar results. Local effects of global warming are often also described well by this non-linear trend. The trend in the Niño3.4 index defined in this way is 0.64 ± 0.18 K/100 ppm (1σ uncertainty) for July–June averages starting in 1900. The trend is independent of the season within uncertainties. This entails a statistically significant rise of 0.8 ± 0.3 K since the late 19th century, in contrast to the SOI without trend.

The most obvious hypothesis is that the SOI index shows that the properties of ENSO have not changed substantially over the last century, but that the Niño3.4 index consists of two components: one describing the dynamics of ENSO and one that slowly rises as the globe warms.

To verify this hypothesis, we analyze whether rainfall teleconnections have changed (figure 1(c)). For this we reconstruct an ENSO index based on the teleconnection to precipitation. First, we compute monthly teleconnection patterns by regressing a global precipitation analysis on the Niño3.4 index $X = \mathrm{regr}(P_d, N_d)$, with P_d the detrended precipitation and N_d the detrended Niño3.4 index. Detrending is defined here as subtracting the regression on the CO_2 concentration as above. Next, we project the analyzed precipitation field on these teleconnection patterns, giving an ENSO index N_p based on whether the observed rainfall patterns coincide with the teleconnections or not: $N_p = X \times P$ (the symbol $\times$ denotes the integral over the product of the fields).

Decomposing the precipitation field into ENSO teleconnections, trends and other variability, $P = XN_d + AC + \varepsilon$, with C the CO_2 concentration that parametrizes the trend, this gives $N_p = X \times XN_d + A \times XC + \varepsilon \times X$, i.e. the precipitation index is proportional to the original detrended index plus a trend term that is determined by how much overlap there is between the precipitation trends A and the ENSO teleconnection pattern X, plus noise. Note that this index is most sensitive to high rainfall areas in the tropics.

We computed this index for a long analysis of precipitation over land, GPCC 2018 (Schneider *et al* 2018), extended with the GPCC monitoring analysis V6 and first guess, 1900–2020. Figure 1(c) shows the series. Except for the first part it strongly resembles the SOI with a factor -1: the correlation over 1950–2020 is $r = -0.94$. Like the SOI it shows no long-term trend over the more reliable part of the record since 1950 (and a non-significant negative trend before that). We verified this result in the CRU TS 4.04 dataset (Harris *et al* 2014) 1901–2019, which has zero trends in the Niño3.4 precipitation index over both the whole century and the period from 1950 (not shown). We also considered an OLR based ENSO index over 1979–2018 (Chiodi and Harrison 2010). This index shows a non-significant trend toward La Niña (not shown).

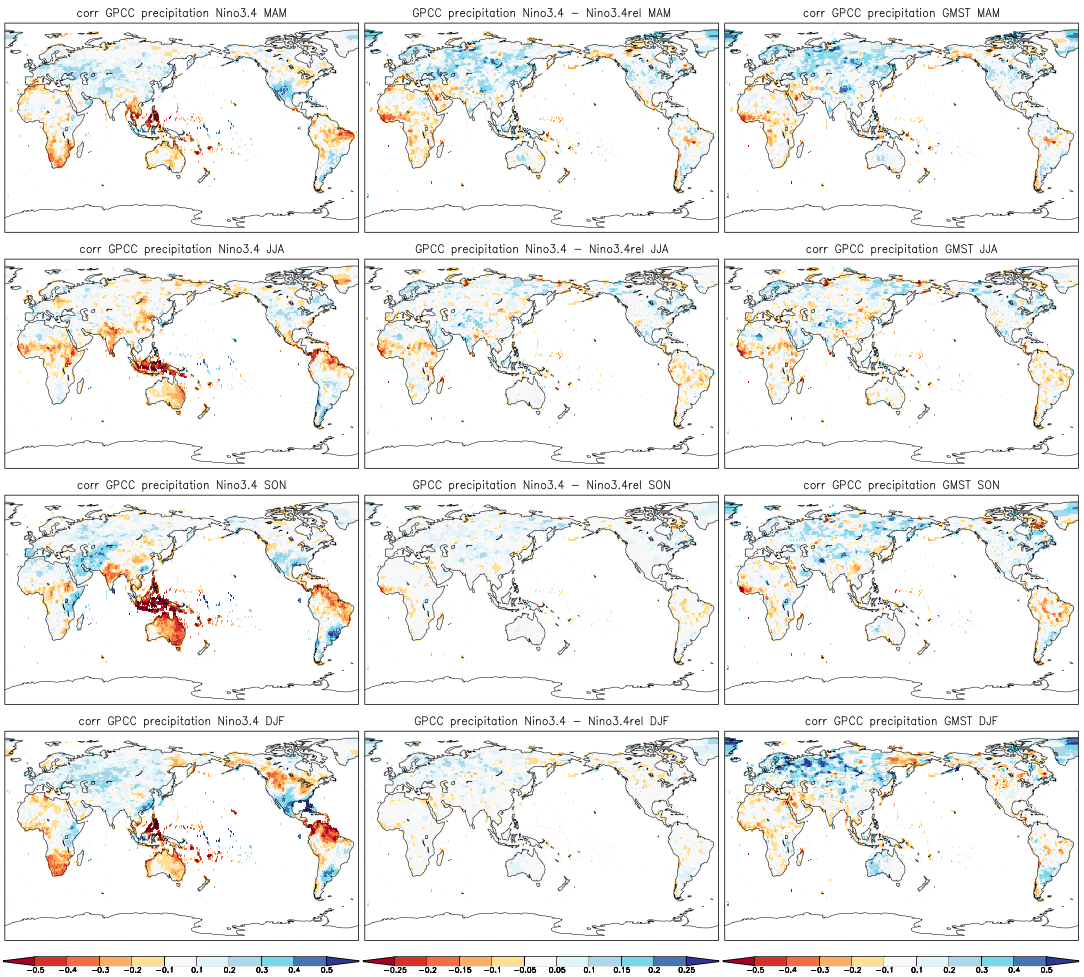

Figure 2. Left: correlation of the Niño3.4 index with GPCC precipitation 1900–2016 (Schneider *et al* 2018) in MAM, JJA, SON and DJF. Middle: difference in correlation with the proposed relative Niño3.4 index. Right: correlation with the global mean temperature (Hansen *et al* 2010).

The same conclusion can be drawn from the spatial structure of the teleconnection patterns. In figure 2 we show the correlation of precipitation with the traditional Niño3.4 index for the four meteorological seasons (left column) and the difference with the correlation with a detrended Niño3.4 index (middle column, see section 4). This difference is very similar to the correlation with the global mean temperature (right column, non-centered field correlations are 0.93–0.94), showing that the correlation maps using the normal Niño3.4 index do not only describe ENSO teleconnections but also have an admixture of global warming trends.

The conclusion is that the traditional Niño3.4 not only describes ENSO but also has a trend due to global warming, which has very different impacts from El Niño. The spatial pattern of the observed SST trend over the past century (figures 1(e) and (f)) also shows that the warming pattern does not resemble the ENSO pattern. This agrees with model projections of ENSO in a warming climate that show no change in the mean state that resembles El Niño or La Niña (e.g. Cai *et al* 2015).

4. A relative Niño3.4 index

Typically, meteorological institutes solve a gradual trend problem by removing monthly averages over the past 30 years, more recently the 1981–2010 period (e.g. Arguez *et al* 2012), although NOAA now shifts the baseline every five years for the Oceanic Niño Index (ONI), which is a 3 month averaged Niño3.4 index. This method has two obvious drawbacks. Every five years there is a small discontinuity of order 0.1 K. Furthermore, the last 10 years cannot be computed in real time as the centered climatology is not yet known, so this correction is applied later. This method thus leaves a remnant of the trend in the Niño3.4 index for the current situation and seasonal forecasts—a problem acknowledged by ENSO forecasters (L'Heureux *et al* 2017).

Another way to separate the trend would be to subtract the regression on an index of global warming, for instance the global mean temperature or CO_2 concentration. However, due to the high variability of ENSO this trend definition has large uncertainties. It

would also change all index values retroactively each year.

We propose to use a a simple but elegant solution to this problem: the relative Niño3.4 index, defined as the difference of the original index with the contemporaneous tropical mean SST anomalies (20° S–20° N as proposed by Johnson and Kosaka (2016)) and shown in figure 1(d). This region has within uncertainties the same trend as the Niño3.4 index (0.90 ± 0.05 K/100 ppm versus 0.64 ± 0.18 K/100 ppm over 1900–2020), so the trends cancel to first order in the difference, although the central value seems to be somewhat overcorrected. The same holds for the Niño1+2, Niño3 and Niño4 indices, so these can be similarly defined. If in the future the trends in the Niño indices diverge from the tropical mean beyond shifts in ENSO this definition will have to be revisited.

As well as effectively removing the trend, subtracting the tropical mean SST results in a relative SST (e.g. Vecchi and Soden 2007, Back and Bretherton 2009, Johnson and Xie 2010, Khodri *et al* 2017, Izumo *et al* 2020) that is of more direct relevance to changes in tropical convection driven by SST anomalies. These SST anomalies promote changes in tropical convection because they cause changes in local static stability, e.g. El Niño anomalies act to warm and moisten the lower troposphere, thus acting to increase precipitating convection over the equatorial central Pacific. However, the resulting tropical upper-tropospheric temperature is approximately uniform in the horizontal (Sobel *et al* 2002) and its value is controlled by the tropical mean SST. A warming (cooling) of the surface that is limited to a small fraction of the tropics (e.g. as occurs during El Niño or La Niña) acts to warm and moisten (cool and dry) the atmospheric boundary layer locally, but does not cause changes of similar magnitude in the free-tropospheric temperature, since the latter must remain approximately uniform horizontally. Such local warming (cooling) thus destabilizes (stabilizes) the overlying atmosphere (Ramsay and Sobel 2011).

In a warming climate, changes in tropical rainfall and even the intensity of tropical cyclones are more sensitive to changes in relative SST than to background warming (Johnson and Xie 2010, Ramsay and Sobel 2011). That is, the pattern of mean SST warming is important because the largest increases in rainfall will occur in the regions that warm the most relative to the tropical mean, referred to as the warmer-get-wetter paradigm (Xie *et al* 2010). Uniform surface warming in the tropics will thus not act to appreciably change the local stability and hence precipitation teleconnections associated with ENSO. It should be noted that the pattern of surface warming that has occurred in the Tropics (figure 1(e)) is different from that expected from increasing greenhouse gases based on climate models, which show maximum warming in the equatorial central Pacific (Cai *et al* 2015). The observed warming has not been uniform so that its effect on ENSO-forced rainfall changes cannot be simply estimated by the local trend in SST. Using relative SST to form the Niño indices will give a much more informative indication of the expected effects on rainfall (figure 2). Note also that relative SST can be used to good effect for other widely used indices of tropical variability such as the Dipole Mode Index in the Indian Ocean.

The relative index also better adjusts for a changing climatology. As one can see in figure 3(a), the NOAA CPC ONI has been substantially warmer, up to about 0.4 °C recently (from 0.2 °C to 0.6 °C in individual months), than a relative ONIs, which uses 30 year climatologies only through 2015. This is comparable with the thresholds used to define El Niño and La Niña, 0.5 °C averaged over three months. The difference in the last 15 years is the consequence of using a lagged climatology, which cannot keep up with the trend.

A technical point is that this index will have a 20% smaller variability than the original Niño3.4 index, as a large part of the interannual variability of the 20° S–20° N series is also ENSO-driven. This is not acceptable for users who rely on fixed categorical thresholds to define events, such as the NOAA thresholds of ±0.5 °C. In addition, statistical models that use the Niño3.4 index would need refitting. We therefore propose to renormalize the series to the same variability as the original Niño3.4 series by multiplying by $1/(1-A)$ with A the regression of the 20° S–20° N SST anomalies on the Niño3.4 index after taking year-on-year differences to isolate the ENSO signal. The regression has a strong seasonal cycle, so it is determined for each month separately (averaging over the two adjoining months in the fit to increase the signal/noise ratio).

5. Explained variance and forecast skill

The relative Niño3.4 index explains 9% less (in MAM) to 1% more (in JJA) of seasonal mean variance of global land precipitation than the normal Niño3.4 index. In DJF the decrease in explained variance is 4% and SON it is 3%. The larger decreases in boreal autumn, winter and spring coincide with the seasons in which there are large trends in precipitation in the high latitudes that are correlated with the trend in the Niño3.4 index (see figure 2). We do not consider this a desirable property of an ENSO index. The explained variance in the tropics is on average the same, 4% less (in MAM) to 2% more (in JJA and DJF) when using the relative index.

Figure 3(b) shows one measure of forecast skill in the ECMWF (old) S4 (Molteni *et al* 2011) and (current) S5 (Johnson *et al* 2018) seasonal forecast systems, the anomaly correlation coefficient at lead +2 months (i.e. the January index forecast from the 1 November analysis etc). The skill in the relative

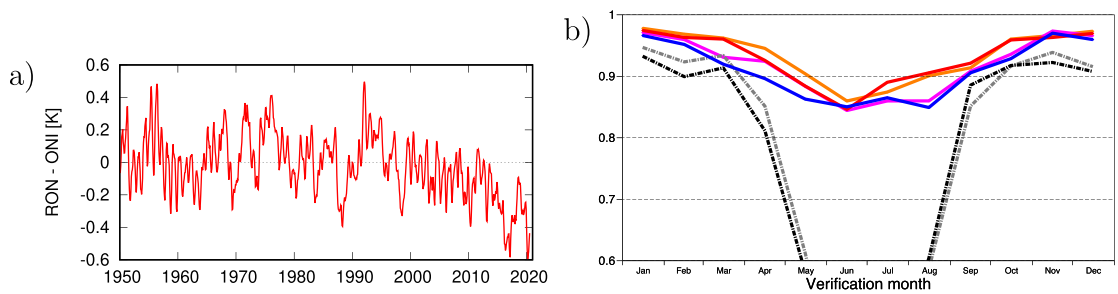

Figure 3. (a) Difference between the relative Ocean Niño Index (ONI) proposed here and the current NOAA/NCEP ONI definition. (b) Anomaly correlation skill score of Niño3.4 indices at two months lead time (i.e. the third month of each forecast) from ECMWF seasonal forecast systems. SEAS5 is shown in red (relative Niño3.4) and orange (Niño3.4), S4 in blue (relative Niño3.4) and purple (Niño3.4). For both models, the choice of index makes only marginal differences to the score. Persistence is shown in black (relative Niño3.4) and grey (Niño3.4).

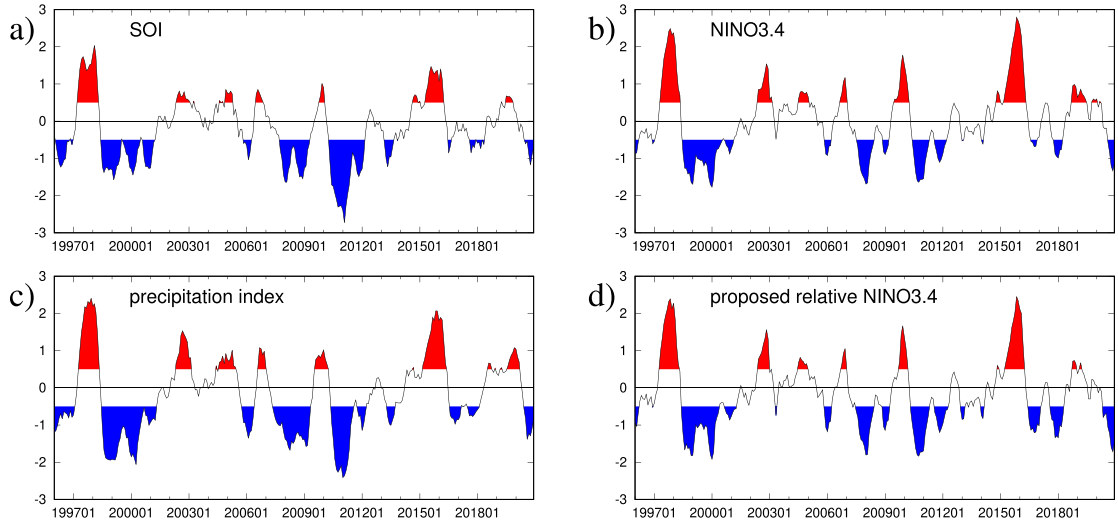

Figure 4. As figure 1 but for monthly indices 1996–2020. The SOI and precipitation indices have been smoothed with a 5 month running mean.

Niño3.4 (red, blue) is slightly lower ($\Delta r \approx 0.3$) than the standard Niño3.4 index (orange, purple) in boreal spring. That time of year the variability is low and therefore the trend contributes more to the skill of the Niño3.4 index forecasts. Removing the trend leaves the proper ENSO teleconnenctions in the interannual variability and hence lowers the skill. The rest of the year the skill measure is very similar or slightly higher ($\Delta r \approx 0.0$ to 0.1). Other lead times give similar results. An official introduction of the relative Niño3.4 index would have to be accompanied with more thorough verification.

6. Implications of a relative index for seasonal preparedness

The use of relative index, which better describes actual ENSO conditions, would have immediate implications for decision-makers. We give a few examples drawn from the last few years.

The ONI index was above 0.5 in the boreal winter of 2014/15, although no major operational ENSO update considered the 2014/15 boreal winter as an El Niño, mostly because the atmospheric response was missing (L'Heureux 2015, McPhaden 2015). There was no clear response in ENSO indices of OLR, winds, etc. The RONI actually clarifies this situation because it classifies 2014/15 as ENSO-neutral. This implies that trends were playing a role in that winter.

In 2015/16 decision-makers, for instance in our East African example, may have over-anticipated, given that the Niño3.4 index indicated an El Niño of unprecedented strength, and warnings referred to potential extreme events and impacts comparable to the intense events of 1997/98 and 1982/83 (neglecting the influences of the Indian Ocean and random weather). Figure 1(d) shows that by using the relative Niño3.4 index there is no evidence that recent El Niño events were much stronger than those in the late 19th and early 20th century. In particular, the 2015/16 event, although squarely in the class of very strong events, is not quite as strong in this measure as the 1997/98 and 1982/83 events. This is also indicated by other ENSO indices (L'Heureux *et al* 2017). The peak monthly absolute Niño3.4 index was higher in 2015/16 (figure 4(b)), but contained a contribution

from global warming of about 0.3 °C relative to 1997/98 and 0.5 °C relative to 1982/83.

Using the relative Niño3.4 index also heavily impacts assessment of the subsequent 2016/17 La Niña (figure 4). The regular Niño3.4 barely reached the −0.5 °C limit that NOAA uses to define La Niña. However, the proposed relative index shows it was a sizeable La Niña, in line with the teleconnections, e.g. heavy precipitation in Indonesia (already noted by Ropelewski and Halpert 1987) and depressed rainfall during the September–November 'short rains' in parts of the Horn of Africa (e.g. Mutai *et al* 1998), which contributed to significant drought conditions. Decision-makers might have been more alert to these risks, especially in the Horn of Africa, had the La Niña signal been more pronounced. It should be noted that direct seasonal forecast of rain correctly indicated a large probability of drought, supported by negative values of the Indian Ocean Dipole index (which also has a trend). This once again shows that only looking at the Niño3.4 index only captures a part of the predictable precipitation signal.

A particular example, directly dependent on the definition of the Niño3.4 index, relates to disaster risk management by the international humanitarian system. Just before the 2016/17 La Niña, the Inter-Agency Standing Committee, the forum for coordination of humanitarian assistance, was in the process of developing a set of standard operating procedures (SOPs) to ensure early action to warning signs of ENSO episodes. These SOPs are triggered at a 55% chance of El Niño or La Niña, which accords to an 'El Niño Watch' status in several forecasting agencies. This then sets in motion a process of vulnerability assessments, mitigation and preparatory actions, based on teleconnections and seasonal forecasts. Because of this threshold for action, the ENSO index plays a critical role in whether or not preparatory actions are taken.

In the case of the 2016/17 La Niña, the definition of the index determines the timing of when the trigger would be reached. The event was defined by NOAA as starting in the July–September season, whereas with the detrended index La Niña would have started in June–August (and would also have ended later). While we do not have a counterfactual of what the consensus forecast would have been in real time during this event, this timeline suggests that stronger probabilities of La Niña would have been available earlier and lasted longer. With increased attention and lead time, greater and earlier action could have been taken to prevent some of the humanitarian impacts of the La Niña teleconnections: greater possibility of drought, which indeed materialized. Adopting the relative Niño3.4 index would also entail that the forecast plumes at various operational seasonal prediction centers would show values that can be compared more directly to the seasonal forecasts via teleconnection patterns than is currently the case. This could reduce misunderstandings such as occurred during the 2016/17 La Niña.

The winter of 2019/20 showed the opposite bias. Using the 1981–2010 climatology, the NCEP ONI definition flagged an El Niño during this season as the ONI was above +0.5 °C for five overlapping seasons. However, the atmospheric state did not show an El Niño state, with the SOI −0.2 averaged over these seasons (figure 4(a)). Satellite-derived precipitation patterns that also cover the sea also did not resemble El Niño teleconnections in the tropics with a second precipitation Niño3.4 index derived from these also only slightly positive (not shown). Restricted to land the teleconnections were El Niño-like (figure 4(c)). The El Niño was so weak that using the relative Niño3.4 index reduced it to neutral during this season. The OLR index of Chiodi and Harrison (2010) also indicated neutral or La Niña conditions (it does not distinguish between these).

It should be noted that ENSO teleconnections are generally weak compared to internal variability. In other specific cases, such as the 2017/18 La Niña the results go the other direction. Recent evidence on food security interventions has urged caution in the humanitarian sector not to overemphasize El Niño events; Choularton and Krishnamurthy (2019) demonstrated that food security predictions for one single location (Ethiopia) were least accurate during the 2015/16 El Niño event. During the 'weak' 2018/19 and 2019/20 events, there were limited humanitarian planning conversations on El Niño.

However, as shown in figure 1 the relative index does on aggregate reduce the bias in ENSO precipitation teleconnections over land and is therefore more useful than the current definition, especially in regions with strong teleconnections. Of course if global warming trends play a role, these should be included, but as a separate index and not mixed in with the ENSO index.

7. Conclusions

Niño3.4 is a widely used index for the strength of El Niño and La Niña, with a better signal/noise ratio than other indices such as the SOI or precipitation-based indices. However, because it is a temperature anomaly, it contains a trend due to global warming. Comparisons with the other indices that more directly monitor the impact of ENSO SST variations on the atmosphere show that this trend is not part of ENSO dynamics.

To remove the trend due to global warming we propose to use the relative Niño3.4 index, constructed by simply subtracting the contemporaneous mean 20° S–20° N SST anomalies, which have within uncertainties the same trend, and rescaling. This relative index also describes the influence of SST on the atmosphere better on theoretical grounds. The relative Niño index can easily be computed in real time

and describes ENSO better than the original index. It can also be forecast by the current seasonal forecast systems with equal or slightly lower skill than the normal Niño3.4 index, with the difference in skill partly due to the absence of common trends. The relative index also better adjusts for a changing climatology. It is available from the KNMI Climate Explorer (climexp.knmi.nl) (van Oldenborgh, 2021).

Using it we find that the 2015/16 El Niño was not stronger than the previous two big ones (1982/83 and 1997/98), and the 2016/17 La Niña was not weak. The 2019/20 El Niño was another example where the Niño3.4 index indicated El Niño, but the atmospheric circulation and the relative Niño3.4 index agree that the situation was closer to neutral.

The use of the relative index should describe teleconnections better, makes it easier to construct statistical seasonal forecast models and explain dynamical model forecasts, and provides a better indication of expected conditions for decision-makers that are trying to manage weather and climate risks in a changing climate. It is also more suited for ENSO research.

Data availability statement

The data that support the findings of this study are openly available at the following URL/DOI: https://climexp.knmi.nl/selectindex.cgi.

ORCID iDs

Geert Jan van Oldenborgh https://orcid.org/0000-0002-6898-9535
Harry Hendon https://orcid.org/0000-0002-4378-2263
Timothy Stockdale https://orcid.org/0000-0002-7901-0337
Michelle L'Heureux https://orcid.org/0000-0002-7095-9706
Erin Coughlan de Perez https://orcid.org/0000-0001-7645-5720
Roop Singh https://orcid.org/0000-0002-6064-9675
Maarten van Aalst https://orcid.org/0000-0003-0319-5627

References

Allan R J, Nicholls N, Jones P D and Butterworth I J 1991 A further extension of the Tahiti-Darwin SOI, early SOI results and Darwin pressure *J. Clim.* **4** 743–9

Arguez A, Durre I, Applequist S, Vose R S, Squires M F, Yin X, Heim R R and Owen T W 2012 NOAA's 1981–2010 U.S. climate normals: an overview *Bull. Am. Meteorol. Soc.* **93** 1687–97

Back L E and Bretherton C S 2009 On the relationship between SST gradients, boundary layer winds and convergence over the Tropical Oceans *J. Clim.* **22** 4182–96

Ballantyne A P, Alden C B, Miller J B, Tans P P and White J W C 2012 Increase in observed net carbon dioxide uptake by land and oceans during the past 50 years *Nature* **488** 70–2

Barnston A G, Chelliah M and Goldenbrg S B 1997 Documentation of a highly ENSO-Related SST Region in the equatorial Pacific *Atmos.-Ocean* **35** 367–83

Cai W *et al* 2015 Increased frequency of extreme La Niña events under greenhouse warming *Nat. Clim. Change* **5** 132–7

Chiodi A M and Harrison D E 2010 Characterizing warm-ENSO variability in the Equatorial Pacific: an OLR perspective *J. Clim.* **23** 2428–39

Choularton R J and Krishnamurthy P K 2019 How accurate is food security early warning? Evaluation of FEWS NET accuracy in Ethiopia *Food Secur.* **11** 333–44

Etheridge D M, Steele L P, Langenfelds R L, Francey R J, Barnola J-M and Morgan V I 1996 Natural and anthropogenic changes in atmospheric CO_2 over the last 1000 years from air in Antarctic ice and firn *J. Geophys. Res. Atmos.* **101** 4115–28

Hansen J, Ruedy R, Sato M and Lo K 2010 Global surface temperature change *Rev. Geophys.* **48** RG4004

Harris I, Jones P D, Osborn T J and Lister D H 2014 Updated high-resolution grids of monthly climatic observations—the CRU TS3.10 dataset *Int. J. Climatol.* **34** 623–42

Horsfall F 2006 Catalogue of indices and definitions of El Nino and La Nina: operational use by WMO members *Technical Report* (World Meteorological Organization Commission for Climatology) (available at: www.wmo.int/pages/prog/wcp/wcasp/documents/ENSO-Indices-Catalogue_12062006.pdf)

Huang B *et al* 2017 Extended reconstructed sea surface temperature, version 5 (ERSSTv5): upgrades, validations and intercomparisons *J. Clim.* **30** 8179–205

Izumo T, Vialard J, Lengaigne M and Suresh I 2020 Relevance of relative sea surface temperature for tropical rainfall interannual variability *Geophys. Res. Lett.* **47** e2019GL086182

Johnson N C and Kosaka Y 2016 The impact of eastern equatorial Pacific convection on the diversity of boreal winter El Niño teleconnection patterns *Clim. Dyn.* **47** 3737–65

Johnson N C and Xie S-P 2010 Changes in the sea surface temperature threshold for tropical convection *Nat. Geosci.* **3** 842–5

Johnson S J *et al* 2018 SEAS5: the new ECMWF seasonal forecast system *Geosci. Model Dev. Discuss.* **12** 1087–17

Khodri M *et al* 2017 Tropical explosive volcanic eruptions can trigger El Niño by cooling tropical Africa *Nat. Commun.* **8** 778

Können G P, Jones P D, Kaltofen M H and Allan R J 1998 Pre-1866 extensions of the Southern oscillations index using early Indonesian and Tahitian meteorological readings *J. Clim.* **11** 2325–39

L'Heureux M L 2015 An overview of the El Niño—Southern Oscillation (ENSO) since 2014 *Science and Technology Infusion Climate Bulletin, NOAA Annual Climate Diagnostics and Prediction Workshop (NOAA's National Weather Service, Denver, CO, USA)* pp 4–7

L'Heureux M L *et al* 2017 Observing and predicting the 2015/16 El Niño *Bull. Am. Meteorol. Soc.* **98** 1363–82

L'Heureux M L, Collins D C and Hu Z-Z 2013 Linear trends in sea surface temperature of the tropical Pacific Ocean and implications for the El Niño-Southern Oscillation *Clim. Dyn.* **40** 1223–36

McPhaden M J 2015 Playing hide and seek with El Niño *Nat. Clim. Change* **5** 791–5

Molteni F, Stockdale T N, Balmaseda M A, Balsamo G, Buizza R, Ferranti L, Magnusson L, Mogensen K, Palmer T N and Vitart F 2011 The new ECMWF seasonal forecast system (System 4) *Technical Report* 656 (Shinfield Park, Reading: ECMWF) (available at: www.ecmwf.int/node/11209)

Mutai C C, Ward M N and Colman A W 1998 Towards the prediction of the East Africa short rains based on sea-surface temperature–atmosphere coupling *Int. J. Climatol.* **18** 975–97

Office for the Coordination of Humanitarian Affairs (OCHA) 2017 Regional outlook for the Horn of Africa and the Great Lakes region

Ramsay H A and Sobel A H 2011 Effects of relative and absolute sea surface temperature on tropical cyclone potential intensity using a single-column model *J. Clim.* **24** 183–93

Rasmusson E M and Carpenter T H 1982 Variations in tropical sea surface temperature and surface wind fields associated with the Southern Oscillation/El Niño *Mon. Wea. Rev.* **110** 354–84

Ropelewski C F and Halpert M S 1987 Global and regional scale precipitation patterns associated with the El Niño/Southern Oscillation *Mon. Wea. Rev.* **115** 1606–26

Schneider U, Becker A, Finger P, Meyer-Christoffer A and Ziese M 2018 *GPCC Full Data Monthly Product Version 2018 at 1.0°: Monthly Land-Surface Precipitation from Rain-Gauges Built on GTS-based and Historical Data* (https://doi.org/10.5676/DWD_GPCC/FD_M_V2018_100)

Sobel A H, Held I M and Bretherton C S 2002 The ENSO signal in tropical tropospheric temperature *J. Clim.* **15** 2702–6

Suckling E B, van Oldenborgh G J, Eden J M and Hawkins E 2016 An empirical model for probabilistic decadal prediction: global attribution and regional hindcasts *Clim. Dyn.* **48** 3115–38

Tippett M K and L'Heureux M L 2020 Low-dimensional representations of Niño 3.4 evolution and the spring persistence barrier *npj Clim. Atmos. Sci.* **3** 24

Uhe P *et al* 2018 Attributing drivers of the 2016 Kenyan drought *Int. J. Climatol.* **38** e554–68

van Oldenborgh G J 2021 Monthly time series, KNMI Climate Explorer (https://climexp.knmi.nl/selectindex.cgi)

van Oldenborgh G J, Balmaseda M A, Ferranti L, Stockdale T N and Anderson D L T 2005 Did the ECMWF seasonal forecast model outperform statistical ENSO forecasts models over the last 15 years? *J. Clim.* **18** 3240–9

Vecchi G A and Soden B J 2007 Effect of remote sea surface temperature change on tropical cyclone potential intensity *Nature* **450** 1066–70

Walker G T 1924 Correlation in seasonal variations of weather IX *Mem. Indian Meteorol. Dep.* **24** 275–332

Xie S-P, Deser C, Vecchi G A, Ma J, Teng H and Wittenberg A T 2010 Global warming pattern formation: sea surface temperature and rainfall *J. Clim.* **23** 966–86